Infinite dilution in doped ceria and high activation energies

Julius Koettgen[a,b,c,d,*], Manfred Martin[a,b,e,f,**]

[a] *Institute of Physical Chemistry, RWTH Aachen University, Landoltweg 2, 52056 Aachen, Germany*
[b] *JARA-HPC, Forschungszentrum Jülich and RWTH Aachen University, Germany*
[c] *Materials Sciences Division, Lawrence Berkeley National Laboratory, Berkeley, California 94720, United States*
[d] *Department of Materials Science and Engineering, University of California, Berkeley, California 94720, United States*
[e] *Helmholtz-Institut Münster (IEK-12), Forschungszentrum Jülich GmbH, Corrensstr. 46, 48149 Münster, Germany*
[f] *JARA-Energy, Forschungszentrum Jülich and RWTH Aachen University, Germany*

ARTICLE INFO

Keywords:
A. Oxides;
D. Defects

Abstract

Oxygen ion diffusion determines the performance of materials in energy conversion, energy storage and catalysis. For nominally pure cerium oxide, experiments measure high activation enthalpies while calculations predict low activation enthalpies. Moreover, for doped oxides, e.g. doped ceria, experiments show a high activation enthalpy for both pure ceria and for high dopant fractions, leading to a minimum in activation enthalpy for small dopant fractions. While for high dopant fractions the increase in activation enthalpy is correlated with the association of oxygen vacancies and dopant ions, which are both created by doping, the minimum in activation enthalpy is assumed in the literature to be related to the maximum in ionic conductivity at similar dopant fractions. In this study, density functional theory (DFT) calculations and Kinetic Monte Carlo (KMC) simulations are combined in order to calculate the ionic conductivity and activation enthalpy in doped oxides. We show that the experimental ionic conductivity and activation energy in nominally pure cerium oxide is dominated by impurities. We resolve the discrepancy between activation enthalpies of nominally pure oxides in experiments as opposed to calculations. This will lead to a more comprehensive understanding of the oxygen ion conductivity and its underlying atomistic mechanisms. Moreover, such a focus will be of great benefit to the future development of sustainable and efficient materials.

This is the Accepted Manuscript version of an article accepted for publication in Solid State Communications. The Version of Record is available online at: https://doi.org/10.1016/j.ssc.2020.113939

Oxygen ion diffusion determines the performance of materials in energy conversion, energy storage and catalysis. The ability to predict ionic conductivities and an improved understanding of the underlying atomistic mechanisms provide important contributions to the future development of sustainable and efficient materials. Though ceria is known for its ability to be easily reduced, leading to an increase in electronic conductivity, experimental and theoretical results confirm that this effect can be neglected for the conditions discussed in the following plan of study.[1] Ionic conductivities in doped ceria have been investigated thoroughly.[2, 3, 4] Despite the importance of the oxygen ion conductivity, calculations are not able to reproduce the ionic conductivity in nominally pure ceria properly as shown in Fig. 1, where the ionic conductivity of Sm doped ceria is shown as a function of the doping fraction for experiments and simulations from our previous work.[4] In fact, oxygen diffusion coefficients of pure ceria vary significantly in nominally pure ceria as shown in Fig. 2 without apparent reason, where a) experimental oxygen vacancy diffusion coefficients of pure ceria as a function of temperature are fitted using an Arrhenius fit and the b) fit parameters are shown.

For a better understanding, these conductivities are separated into a pre-exponential factor A and activation enthalpy ΔH_a according to an Arrhenius behavior:

$$\sigma = \frac{A}{T} e^{-\frac{\Delta H_\mathrm{a}}{k_\mathrm{B} T}} . \tag{1}$$

Experiments show a high activation enthalpy both for pure ceria[1] and for high dopant fractions,[2, 3, 4] leading to a minimum in activation enthalpy for small dopant fractions. While for high dopant fractions the increase in activation

---

[*] Corresponding author
[**] Principal corresponding author

✉ `julius.koettgen@rwth-aachen.de` (J. Koettgen); `martin@rwth-aachen.de` (M. Martin)
ORCID(s): `0000-0002-8260-4793` (J. Koettgen); `0000-0001-9046-050X` (M. Martin)

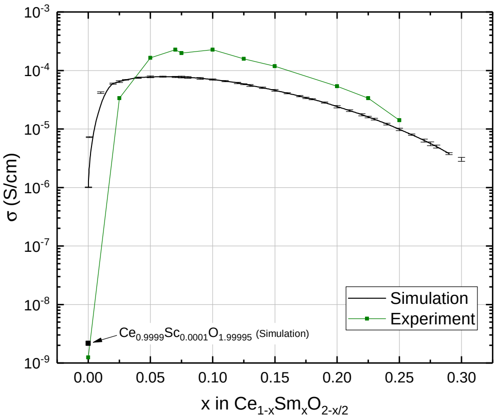

Figure 1: Comparison of simulated and experimental ionic conductivity as a function of doping fraction. Sm doped ceria was investigated at 267 °C. Bulk ionic conductivities according to own impedance experiments are shown. Additionally, the simulated ionic conductivity of $Ce_{0.9999}Sc_{0.0001}O_{1.99995}$ is shown. Lines are a guide to the eye only.[4] - Reproduced by permission of the PCCP Owner Societies

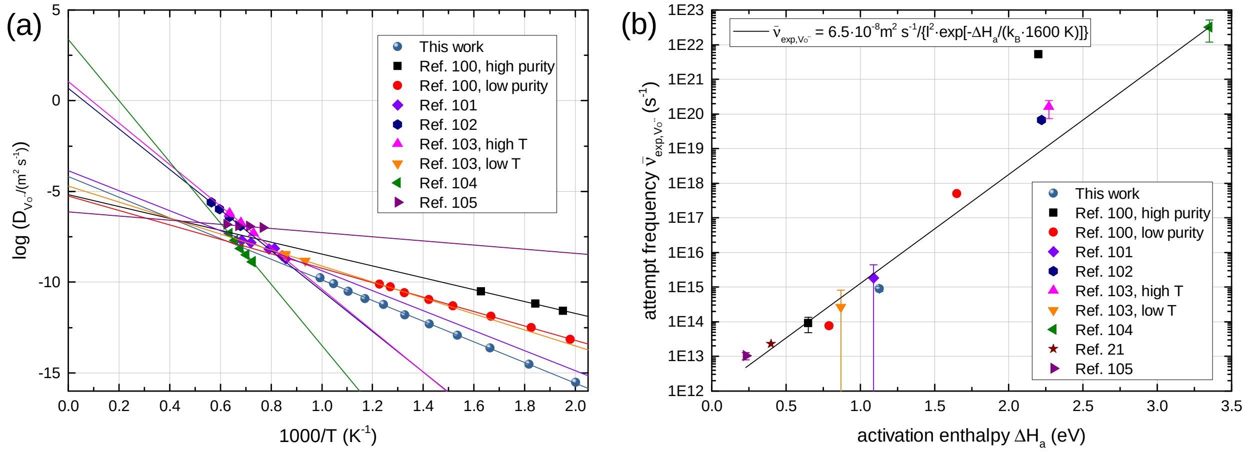

Figure 2: Experimental (a) oxygen vacancy diffusion coefficients and (b) resulting attempt frequencies of pure ceria using bulk[5] and total[6, 7, 8, 9, 10, 11] domain. Though experimental attempt frequencies vary over several orders of magnitude, all experiments are probably based on the same elemental frequency for a jump process.[1] - Reproduced by permission of the PCCP Owner Societies

enthalpy is correlated with the association of oxygen vacancies and dopant ions, which are both created by doping, the minimum in activation enthalpy is assumed in literature to be related to the maximum in ionic conductivity at similar dopant fractions. Experiments show for Y doped ceria an activation enthalpy minimum between room temperature and 330 °C,[2] or higher temperatures up to 700 °C.[3]

Ionic conductivities are calculated in order to understand known materials and predict properties for the design of new materials. The direct computation of diffusion coefficients for dilute defects is possible using *ab initio* methods.[12] In this study, density functional theory (DFT) calculations and Kinetic Monte Carlo (KMC) simulations are combined to calculate the ionic conductivity in doped oxides in accordance with an earlier work.[4] This framework is the improved result based on both works in literature[13, 14, 15, 16, 17, 18] and own previous works[19, 1, 20] and improved the prediction of diffusion compared to previous theoretical studies.[4] In this framework, experimental ionic conductivities in doped ceria were successfully reproduced using a first principles study. Similar to the procedure in experimental literature, an activation enthalpy ΔH_a for an Arrhenius behavior can be extracted. While the increase in activation enthalpy for increasing dopant fractions is successfully reproduced, the simulation of pure ceria results in a ΔH_a that is equal to the low migration energy in pure diluted ceria. This result is in agreement with the common

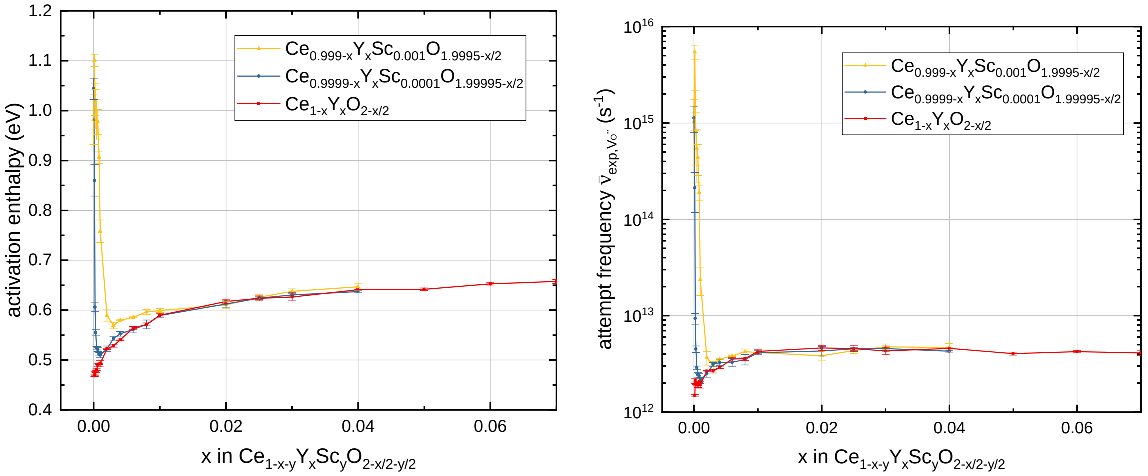

Figure 3: Simulated activation enthalpy (left) and attempt frequency (right) in Y-doped and Sc-Y-co-doped ceria as a function of the dopant fraction. Kinetic Monte Carlo (KMC) simulations using input parameters from density functional theory (DFT) were performed in 25 °C steps between 500 and 600 °C. The activation enthalpy and attempt frequency were extracted according to Eq. 1. Lines are guide to the eye only.

understanding in literature, but contrasts with the experimental results for the ionic conductivity as well as the Arrhenius behavior including the pre-factor of diffusion (the jump attempt frequency) and the activation enthalpy.[4] In the following, we will show a possibility to resolve the discrepancy between activation enthalpies of nominally pure oxides in experiments as opposed to calculations.

Possible reasons for varying activation were already discussed in both the computational and experimental aspects of an earlier work.[1] Minor influences in experiments include measuring inaccuracies and technique. Major influences include sample properties like afore mentioned possible reduction of ceria and the macroscopic structure composed of bulk and grain boundaries. Additionally, experiments show that the activation enthalpy is strongly influenced by the chosen temperature range.[3] Computational errors include both minor error due to the chosen computational parameters, and major error due to methodical approximations such as: 1) the change in lattice parameter due to doping and thermal expansion, and 2) the neglect of return jumps and anharmonicity effects due to the harmonic approximation in the transition state theory. These errors were also investigated in earlier works.[1, 20, 4] Neither of these computational and experimental influences is found to be sufficient to explain the discrepancy between activation enthalpies in experiments versus calculations.

In nominally pure oxides, experiments and calculations differ, beyond the influences discussed above, in another important way. While calculations easily can investigate infinitely diluted defects, samples in experiments can contain significant amounts of impurities.[1, 7, 21] Experiments show a significant influence of the concentration of impurities.[3] Therefore, it would be consistent to include these impurities in the calculations, even though often in literature, no defect interactions for small dopant concentrations are expected.[1, 4] Figure 3 (left) shows the simulation of the activation enthalpy as a function of the dopant fraction for common experimental concentrations of impurities derived from an Arrhenius fit of the conductivities for 500, 525, 550, 575, and 600 °C. As the chemical composition of impurities varies in the literature, we choose to demonstrate the influence of impurities with a rare-earth dopant that has strong trapping properties, i.e. a dopant that mitigates migration of oxygen vacancies to the dopant but impedes jumps away from the dopant. From the dopants investigated in our earlier work, we choose the dopant Sc, which has strong trapping properties.[4] The activation enthalpy was extracted in accordance with experiments using Eq. 1. For the Arrhenius relationship according to Eq. 1, it was assumed that the mechanical mobility b_i, given by $\sigma_i = n_i \cdot z_i^2 e^2 \cdot b_i$ as well as the squared charge and concentration of the charge carriers, is related to the diffusion coefficient D_i by the classical Einstein relation ($b_i = \frac{D_i}{k_B T}$). This is true for defects, which do not interact with each other and, therefore, do not influence the diffusion of oxygen, but inaccurate for doped materials. Additionally, the relationships shows that the pre-exponential factor is given by the jump distance and a mean experimental attempt frequency according to $D_i = l^2 \cdot \overline{\nu}_{\mathrm{exp},i} \cdot e^{-\frac{\Delta H_\mathrm{a}}{k_\mathrm{B} T}}$. Temperatures between 500 and 600 °C are investigated. For the calculation of the attempt fre-

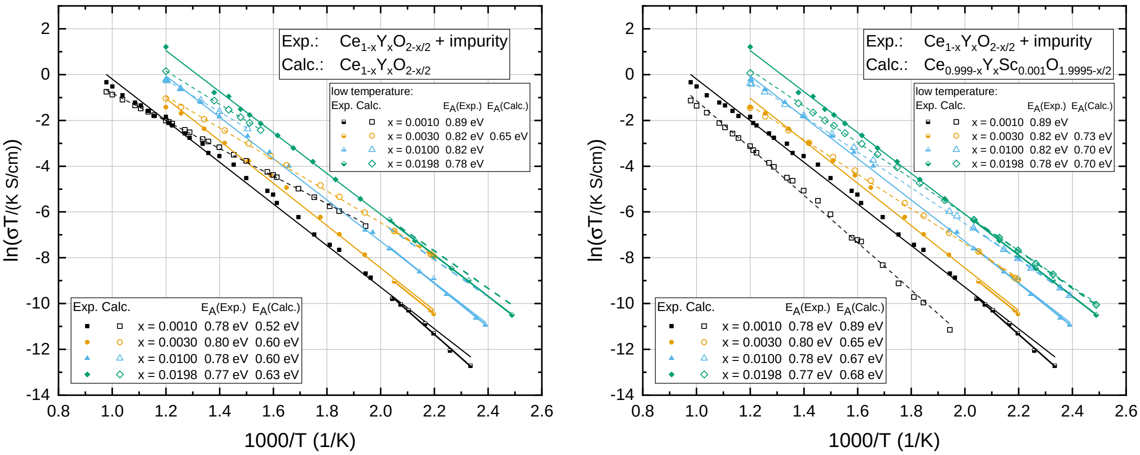

Figure 4: Simulated ionic conductivity and activation enthalpy in Y-doped (left) and Sc-Y-co-doped ceria (right). Experiments according to Wang *et al.* are shown as a comparison.[3]

quency in Fig. 3 (right) only the concentration of yttrium was considered according to the experiment. The simulated activation enthalpies in Y-doped and Sc-Y-co-doped ceria show a substantial influence of impurities on the activation enthalpy for small overall dopant fractions. Therefore, we believe that impurities dominate both ionic conductivities and activation enthalpies of selected nominally pure oxides.

Figure 3, where simulated ionic conductivity in Y-doped (left) and Sc-Y-co-doped ceria (right) are compared with experiments according to Wang *et al.*,[3] shows for Sc-Y-co-doped ceria that with increasing dopant fractions, activation enthalpies first decrease then subsequently increase. In this way, a minimum in activation enthalpy is simulated, as found in the experiments. This result is of significant importance, and not only in relation to predicting correct diffusion coefficients and activation enthalpies of nominally pure materials. Moreover, the minimum in activation enthalpy found in experiments as a function of doping concentration was correlated with the maximum in ionic conductivity measured beforehand. The presented results suggest that this common interpretation in literature is flawed. In fact, the minimum in activation enthalpy is the result of impurity dominated materials.

Figure 4 (left) show the ionic conductivity and activation enthalpy in Y-doped ceria according to Wang *et al.*[3] Again, calculations of pure Y-doped ceria cannot reproduce the activation energy minimum found in experiments. Moreover, simulated ionic conductivity and activation enthalpy significantly deviate from experimental results. Figure 4 (right) show the ionic conductivity and activation enthalpy in co-Sc-Y-doped ceria. According to the experiments of Wang *et al.*[3], impurities levels are considered and assumed to be Sc for simplicity. Considering 0.1 % impurities leads to significant improvement in the agreement between calculations and experiments.

In this work, we show that the experimental ionic conductivity and activation energy in nominally pure cerium oxide is dominated by impurities. We resolve the discrepancy between activation enthalpies of nominally pure oxides in experiments as opposed to calculations. In this way, the oxygen ion conductivity and its underlying atomistic mechanisms will become better understood. Moreover, future development of sustainable and efficient materials will be significantly improved.

Acknowledgments

The authors gratefully acknowledge the computing time granted by the JARA-HPC Vergabegremium and provided on the JARA-HPC Partition part of the supercomputer JURECA at Forschungszentrum Jülich.[22] Simulations were performed with computing resources granted by RWTH Aachen University under project rwth0336. The authors gratefully acknowledge the computing time granted by the JARA-HPC Vergabegremium and provided on the JARA-HPC Partition part of the supercomputer CLAIX at RWTH Aachen University. Research supported by the U.S. Department of Energy, Office of Science, Basic Energy Sciences, Materials Sciences and Engineering Division under Contract No. DE-AC02-05-CH11231. Discussions with Long-Qing Chen are gratefully acknowledged.

Appendix: Computational details

Ab initio calculations were performed using the density functional theory (DFT) in the Generalized Gradient Approximation (GGA) according to Perdew, Burke and Ernzerhof (PBE)[23] and the projector augmented-wave method (PAW)[24] in the Vienna Ab initio Simulation Package (VASP).[25, 26] An energy cut-off of 500 eV for the plane waves was selected. Supercells consisting of $2\times2\times2$, $3\times3\times3$ and $4\times4\times4$ unit cells were calculated. Subsequently, the electrostatic energy created by periodic boundary conditions was corrected according Makov and Payne.[27, 4] Monkhorst-Pack k-point meshes of $2\times2\times2$ for the $2\times2\times2$ supercell and $1\times1\times1$ for larger supercells were investigated.[4]

As valence electrons, $5s^2 5p^6 6s^2 5d^1 4f^1$ for cerium atoms, $3s^2 3p^6 3d^1 4s^2$ for scandium atoms, and $4s^2 4p^6 4d^1 5s^2$ for yttrium atoms were used. A Hubbard U parameter ($U = 5$ eV for the 4f-orbitals of cerium) was introduced by the rotational invariant approach to account for the localization of strongly correlated f-electrons[28] in agreement with literature.[29, 30, 31, 32, 33, 34, 35, 36, 37] Charge-neutral cells are divided into oppositely charged cells and are calculated by assuming a neutralizing background charge, which is a valid approach as shown in literature.[38, 39, 40, 41] Convergence parameters for electronic and ionic relaxation are at least 10^{-5} eV and 10^{-2} eV/Å, respectively.[4]

A lattice constant for defect-free ceria was calculated using the Birch-Murnaghan equation of state (5.49 Å, larger than in experiments due to the chosen set of parameters)[42, 43, 44] and applied for all stoichiometries as performed in literature.[45, 46, 47] Atomic positions are always optimized.[4]

The interaction (association or repulsion) energy between defects (oxygen vacancies V and dopant cations RE) are calculated by placing defects on regular lattice sites up to distance of about 5.5 Å and comparing their energy for V-V and RE-V interactions. Migration barriers were calculated using the nudged elastic band method (NEB)[48, 49, 50] by optimizing an interpolated transition state. No difference was found to calculations with several interpolated intermediate images as well as the climbing image nudged elastic band method (CI-NEB).[51] In fluorite-structured ceria, the migration of oxygen vacancies is considered between adjacent tetrahedral oxygen sites in (100) direction. Along this pathway two cations form a 'migration edge' through which the migrating oxygen has to pass. Migration barriers E_{edge} are calculated for a migration edge with two Ce ions, one Ce and one rare-earth ion and two rare-earth ions. All further migration barriers are modeled by combining the difference in interaction energies, which is calculated as a sum of all interactions for initial and final position $\Delta E_{\text{interact}}$, with the calculated migration edges according to $E_{\text{mig},i,j} = E_{\text{edge}} + 0.5\Delta E_{\text{interact}}$.[4]

Oxygen ion conductivity in ceria can be calculated using Kinetic Monte Carlo (KMC) simulations.[13, 52, 14, 53, 54] KMC simulations simulate kinetic processes dynamically from state to state.[55, 13] Jumps surmounted energy barriers $E_{\text{mig},i,j}$ with a transition rate of $\Gamma_{i,j} = \nu_{0,i,j} \cdot \exp\left(-\Delta E_{\text{mig},i,j} / \left(k_{\text{B}} T\right)\right)$ with the attempt frequency $\nu_{0,i,j} = 1.47 \cdot 10^{12}\ \text{s}^{-1}$, which was calculated in an earlier work.[1] An fluorite-structured lattice with a cation- and anion sublattice is created ($16\times16\times16$ supercell with 49152 ions or vacancies and periodic boundary conditions) and filled randomly according to $\text{RE}_2\text{O}_3 \longrightarrow 2\,\text{RE}_{\text{Ce}}' + 3\,\text{O}_{\text{O}}^{\times} + \text{V}_{\text{O}}^{\bullet\bullet}$ with cerium or dopant ions and oxygen ions or oxygen vacancies, respectively. An oxygen vacancy and jump direction is randomly chosen and the jump is performed in case that a random number in the interval [0,1[is smaller than the Boltzmann probability $p_{i,j} = \exp\left(-\Delta E_{\text{mig},i,j} / \left(k_{\text{B}} T\right)\right)$. This is repeated with the number of jump attempts N_{att} until a specified number of jumps is performed (Monte Carlo steps per particle, here: oxygen ion).[56] The mean displacement of all oxygen ions $\langle x \rangle$ is calculated using $\sigma = \frac{\langle x \rangle}{\epsilon_x t} q n_{\text{V}}$ where $\epsilon_x = 0.1 \frac{k_{\text{B}} T}{q l}$ is the strength of the electric field that is applied, l is the jump distance and q and n_{V} are the charge and concentration of the oxygen vacancies, respectively.[57, 58, 59, 19] Test verified that the electric field does not influence the thermodynamic equilibrium and the conductivity is isotropic.[4] The resulting time span is calculated as $t = N_{\text{att}} / \left(6 N_{\text{V}} \cdot \nu_{0,\text{i,j}}\right)$ with the number of oxygen vacancies N_{V}.[60] At the beginning, anion sublattices were at first equilibrated by 100 Monte Carlo Steps per particle. Simulations of the ionic conductivity were repeated at least ten times each with 100 Monte Carlo Steps per particle. The standard error on the conductivity results primarily from the use of different starting lattices.[4]

For temperatures below 360 °C, lattices were equilibrated at higher temperature, and subsequently only 10 Monte Carlo Steps per particle for equilibration were used. Additionally, the number of accepted jumps is increased: Jump probabilities are increased by a factor A so that the most probable transition, which has at least 100 jump attempts cumulated with more probable transitions within 10^9 total jump attempts, has the probability 1 without any detected loss in accuracy. The simulated physical time span is multiplied with A.[4]

References

[1] J. Koettgen, T. Zacherle, S. Grieshammer and M. Martin, *Physical Chemistry Chemical Physics*, 2017, **19**, 9957–9973.
[2] J. Faber, C. Geoffroy, A. Roux, A. Sylvestre and P. Abélard, *Applied Physics A Solids and Surfaces*, 1989, **49**, 225–232.
[3] D. Wang, D. Park, J. Griffith and A. Nowick, *Solid State Ionics*, 1981, **2**, 95–105.
[4] J. Koettgen, S. Grieshammer, P. Hein, B. O. H. Grope, M. Nakayama and M. Martin, *Physical Chemistry Chemical Physics*, 2018, **20**, 14291–14321.
[5] D. Y. Wang and A. S. Nowick, *Journal of Solid State Chemistry*, 1980, **35**, 325–333.
[6] J. M. Floyd, *Indian J. Tech.*, 1973, **11**, 589–594.
[7] F. S. Brugner and R. N. Blumenthal, *Journal of the American Ceramic Society*, 1971, **54**, 57.
[8] M. Kamiya, E. Shimada, Y. Ikuma, M. Komatsu and H. Haneda, *Journal of The Electrochemical Society*, 2000, **147**, 1222.
[9] M. Kamiya, E. Shimada and Y. Ikuma, *Journal of the Ceramic Society of Japan*, 1998, **106**, 1023–1026.
[10] H. Tuller and A. Nowick, *Journal of Physics and Chemistry of Solids*, 1977, **38**, 859–867.
[11] I. K. Naik and T. Y. Tien, *Journal of Physics and Chemistry of Solids*, 1978, **39**, 311–315.
[12] M. Mantina, Y. Wang, R. Arroyave, S. L. Shang, L. Q. Chen and Z. K. Liu, *Journal of Physics: Condensed Matter*, 2012, **24**, 305402.
[13] A. Murray, G. Murch and C. Catlow, *Solid State Ionics*, 1986, **18-19**, 196–202.
[14] M. Meyer and N. Nicoloso, *Berichte der Bunsen-Gesellschaft*, 1997, **101**, 1393–1398.
[15] R. Krishnamurthy, Y.-G. Yoon, D. J. Srolovitz and R. Car, *Journal of the American Ceramic Society*, 2004, **87**, 1821–1830.
[16] R. Pornprasertsuk, P. Ramanarayanan, C. B. Musgrave and F. B. Prinz, *Journal of Applied Physics*, 2005, **98**, 103513.
[17] R. Pornprasertsuk, J. Cheng, H. Huang and F. B. Printz, *Solid State Ionics*, 2007, **178**, 195–205.
[18] M. Nakayama and M. Martin, *Physical Chemistry Chemical Physics*, 2009, **11**, 3241–3249.
[19] S. Grieshammer, B. O. H. Grope, J. Koettgen and M. Martin, *Physical Chemistry Chemical Physics*, 2014, **16**, 9974.
[20] J. Koettgen, P. C. Schmidt, T. Bučko and M. Martin, *Physical Review B*, 2018, **97**, 024305.
[21] R. N. Blumenthal, P. W. Lee and R. J. Panlener, *Journal of The Electrochemical Society*, 1971, **118**, 123.
[22] Jülich Supercomputing Centre, *Journal of large-scale research facilities*, 2016, **2**, A62.
[23] J. P. Perdew, K. Burke and M. Ernzerhof, *Physical Review Letters*, 1997, **78**, 1396.
[24] P. E. Blöchl, *Physical Review B*, 1994, **50**, 17953–17979.
[25] G. Kresse and J. Furthmüller, *Physical Review B*, 1996, **54**, 11169–11186.
[26] G. Kresse and D. Joubert, *Physical Review B*, 1999, **59**, 1758–1775.
[27] G. Makov and M. C. Payne, *Physical Review B*, 1995, **51**, 4014–4022.
[28] S. L. Dudarev, G. A. Botton, S. Y. Savrasov, C. J. Humphreys and A. P. Sutton, *Physical Review B*, 1998, **57**, 1505–1509.
[29] M. Nolan and J. E. W. G. W. Fearon, *Solid State Ionics*, 2006, **177**, 3069–3074.
[30] Z. Yang, G. Luo, Z. Lu and K. Hermansson, *The Journal of Chemical Physics*, 2007, **127**, 074704.
[31] Z. Yang, G. Luo, Z. Lu, T. K. Woo and K. Hermansson, *Journal of Physics: Condensed Matter*, 2008, **20**, 035210.
[32] M. Nolan, V. S. Verdugo and H. Metiu, *Surface Science*, 2008, **602**, 2734–2742.
[33] J. Hooper, A. Ismail, J. B. Giorgi and T. K. Woo, *Physical Chemistry Chemical Physics*, 2010, **12**, 12969.
[34] P. P. Dholabhai, J. B. Adams, P. Crozier and R. Sharma, *Physical Chemistry Chemical Physics*, 2010, **12**, 7904.
[35] P. P. Dholabhai, J. B. Adams, P. Crozier and R. Sharma, *The Journal of Chemical Physics*, 2010, **132**, 094104.
[36] A. Ismail, J. Hooper, J. B. Giorgi and T. K. Woo, *Physical Chemistry Chemical Physics*, 2011, **13**, 6116.
[37] P. P. Dholabhai and J. B. Adams, *Journal of Materials Science*, 2012, **47**, 7530–7541.
[38] T. Zacherle, P. C. Schmidt and M. Martin, *Physical Review B*, 2013, **87**, 235206.
[39] J. X. Zheng, G. Ceder, T. Maxisch, W. K. Chim and W. K. Choi, *Physical Review B*, 2006, **73**, 104101.
[40] J. Wang, Y. Du, H. Xu, C. Jiang, Y. Kong, L. Sun and Z.-K. Liu, *Physical Review B*, 2011, **84**, 024107.
[41] X. Li, M. W. Finnis, J. He, R. K. Behera, S. R. Phillpot, S. B. Sinnott and E. C. Dickey, *Acta Materialia*, 2009, **57**, 5882–5891.
[42] F. D. Murnaghan, *American Journal of Mathematics*, 1937, **59**, 235.
[43] F. D. Murnaghan, *Proceedings of the National Academy of Sciences*, 1944, **30**, 244–247.
[44] F. Birch, *Physical Review*, 1947, **71**, 809–824.
[45] J. L. F. Da Silva, M. V. Ganduglia-Pirovano, J. Sauer, V. Bayer and G. Kresse, *Physical Review B*, 2007, **75**, 045121.
[46] P. R. L. Keating, D. O. Scanlon, B. J. Morgan, N. M. Galea and G. W. Watson, *The Journal of Physical Chemistry C*, 2012, **116**, 2443–2452.
[47] T. Zacherle, A. Schriever, R. A. De Souza and M. Martin, *Physical Review B*, 2013, **87**, 134104.
[48] G. Mills, H. Jónsson and G. K. Schenter, *Surface Science*, 1995, **324**, 305–337.
[49] H. Jonsson, G. Mills and K. M. Jacobsen, in *Classical and quantum dynamics in condensed phase simulations*, ed. B. J. Berne, World Scientific, Singapore, 1998, pp. 385–404.
[50] M. Lumeij, J. Koettgen, M. Gilleßen, T. Itoh and R. Dronskowski, *Solid State Ionics*, 2012, **222-223**, 53–58.
[51] G. Henkelman, B. P. Uberuaga and H. Jónsson, *The Journal of Chemical Physics*, 2000, **113**, 9901.
[52] S. B. Adler and J. W. Smith, *Journal of the Chemical Society, Faraday Transactions*, 1993, **89**, 3123.
[53] A. Oaks, Di Yun, B. Ye, W.-Y. Chen and J. F. Stubbins, *Journal of Nuclear Materials*, 2011, **414**, 145–149.
[54] P. P. Dholabhai, S. Anwar, J. B. Adams, P. Crozier and R. Sharma, *Journal of Solid State Chemistry*, 2011, **184**, 811–817.
[55] G. E. Murch, *American Journal of Physics*, 1979, **47**, 78.
[56] S. L. Lin and J. N. Bardsley, *Computer Physics Communications*, 1978, **15**, 161–163.
[57] W. Visscher, *Physical Review A*, 1974, **10**, 2461–2472.
[58] G. E. Murch and R. J. Thorn, *Philosophical Magazine*, 1977, **36**, 529–539.
[59] G. Murch, *Solid State Ionics*, 1982, **7**, 177–198.
[60] A. F. Voter, in *Radiation effects in solids*, ed. K. E. Sickafus, E. A. Kotomin and B. P. Uberuaga, Springer, Dordrecht, 2007, vol. 235, pp. 1–23.